This article has been accepted for inclusion in a future issue of this journal. Content is final as presented, with the exception of pagination.

An Internet-Inspired Proportional Fair EV Charging Control Method

Emin Ucer, *Student Member, IEEE*, Mithat C. Kisacikoglu, *Member, IEEE*,
Murat Yuksel, *Senior Member, IEEE*, and Ali Cafer Gurbuz, *Senior Member, IEEE*

***Abstract*—Transportation systems are undergoing a major transition with the integration of electric vehicles (EVs). However, due to increase in battery energy and charger power ratings, potential adverse effects on the distribution grid is a crucial issue to be addressed. Large voltage drops at charging nodes will deteriorate the quality of power service and cause unfair utilization of grid capacity among EV users. Safe and efficient operation of the grid along with a fast, convenient, and fair charging strategy is an important research problem. In this paper, we adapt the additive increase multiplicative decrease (AIMD) algorithm used in the Internet congestion control to EV charging using only local node measurements. We analyze the relationship between distance and grid voltage, and show how to extract this information from local measurements. Then, we present a detailed analysis to understand the relationship between distance and charging power in a distribution network to better address the fairness in the proposed AIMD EV charging algorithm. Results show that localized information at charging node voltages include important signature information on grid congestion and can be used to implement AIMD control for EV charging.**

***Index Terms*—Charging stations, complex networks, computer networks, distributed managament, electric vehicles, power distribution, smart grids, TCPIP.**

I. Introduction

ELECTRIC vehicles (EVs) are expected to become an important factor in modern transportation systems. Their reduced CO_2 emissions, efficient operation, increased performance, and lower maintenance requirement make them an attractive candidate for customers. With decreasing prices, EVs will become competitive and are expected to ramp up in sales by 2025 [1]. However, traditional electric utility grid operation is still not ready for this transition [2]. Such a potential mass EV integration brings new challenges in the distribution grid, such as severe voltage drops and deviations, power losses, and frequent peak loads, which are extensively studied in the literature [3]–[10].

Manuscript received June 27, 2018; revised December 8, 2018; accepted February 12, 2019. This work was supported by the National Science Foundation under Award 1755996. *(Corresponding author: Mithat C. Kisacikoglu.)*

E. Ucer and M. C. Kisacikoglu are with the Department of Electrical and Computer Engineering, University of Alabama, Tuscaloosa, AL 35487 USA (e-mail: eucer@crimson.ua.edu; mkisacik@ua.edu).

M. Yuksel is with the Department of Electrical and Computer Engineering, University of Central Florida, Orlando, FL 32816 USA (e-mail: murat.yuksel@ucf.edu).

A. C. Gurbuz is with the Department of Electrical and Computer Engineering, Mississippi State University, Mississippi State, MS 39762 USA (e-mail: gurbuz@ece.msstate.edu).

Digital Object Identifier 10.1109/JSYST.2019.2903835

To mitigate the adverse effects of EV grid integration (EVGI), various EV charging/discharging solutions have been proposed. The charging solutions can be divided into direct, indirect, and autonomous methods [11]. Direct and indirect methods require extensive amount of data exchange between EV and the grid, e.g., battery state of charge (SOC), vehicle arrival and departure times, grid congestion signals, price tariffs [12]. These signals are used to decide or influence when a customer charges an EV. However, they require new installments of expensive communication devices at every node. The conventional wisdom has been that these techniques are a more reasonable way of integrating EVs to the grid, however, cost efficiency as well as deployment practicality at massive scales are questionable.

Furthermore, advanced integration solutions with vehicle-to-grid power transfer are also proposed including load leveling, peak shaving, voltage regulation, and reactive power compensation [13]–[17]. These solutions require a centralized server that can exchange information with end nodes to optimize the operation of EV charging. Considering the additional communication network complexity, its inherent limitations (e.g., latency, loss of data, connection problems), and the required investment costs, centralized solutions are more demanding to implement than distributed methods.

Similar to the EV charging network, the Internet's backbone network carrying data traffic also faced congestion control challenges in the past. As the count of endpoints boomed in the Internet, scalable control of the congestion with easy deployment to practice was a major challenge [18]. Practical observation of the "congestion collapse" [19], [20] necessitated solutions that guarantee stability of the network by avoiding congestion [21] while maximizing the end-to-end (E2E) throughput and making sure the network's capacity is used fairly and efficiently. Due to the multiprovider nature of the Internet as well as the scale complexity of the problem, the solution has been best realized at smart endpoints operating with entirely E2E and local measurements. The mainstream transport protocol TCP adopted this decentralized E2E congestion control approach [22]. Although significant effort has also been spent in centralized [23] and network-supported [24] congestion control for more efficiency and regulated fair usage of the network capacity, most of them stayed at network edges with limited deployments unable to span multiple providers. Decentralized designs with smart endpoints and local/E2E measurements have been the most successful in penetrating into practice and solving the congestion (or data traffic rate) control problem at large scales.

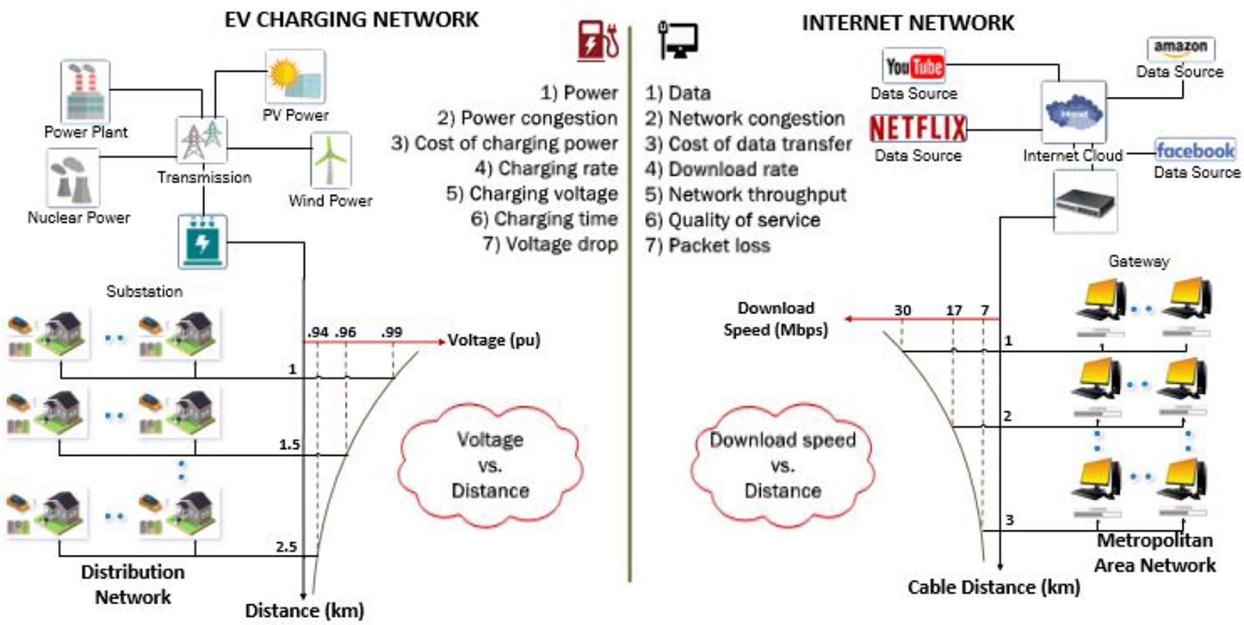

Fig. 1. Analogy between EV charging over the distribution grid and the downloads over the Internet.

Many control methods were proposed and studied, yet only one was widely adopted in the Internet congestion control. This de-facto congestion control uses the additive increase multiplicative decrease (AIMD) algorithm [21], which is basically an event-triggered mechanism that takes some control actions when a congestion in the network occurs. In summary, every end node in the network increases their share linearly in an additive fashion until a congestion occurs in the network. Then, they back up by reducing their share multiplicatively and free up the resource (i.e., the capacity of the links) for reallocation. The congestion level is determined by a threshold time it takes to get an acknowledgment of whether a data packet has reached its destination, a.k.a. round-trip time. This decentralized learning mechanism provides partial information regarding the congestion that may exist in the middle of the network. Such a straightforward solution has proved itself to be stable and maintain proportional fairness among users [25]. A lot of work has been done regarding the AIMD's modeling, operational mechanism, stability, fairness, and different variations. Interested readers might find some of these useful references in [26]–[29]. The AIMD algorithm proposed in this study is described in detail in Section IV-A.

Because of the similarities between the EV charging control and the Internet's source data rate control (see Fig. 1), studies tried to adopt the AIMD algorithm to EV charging [30]–[32]. This idea was further enhanced by taking power system constraints into account [33]. The effects of an AIMD-based algorithm on the distribution system dynamics are presented in [34]. The authors in [35] present a comparison between two AIMD-based charging algorithms and an ideal centralized solution to benchmark the performance on a low voltage distribution network. AIMD approach is also used to solve the share of power generation problems among distributed energy sources in microgrids [36]. In [37], the authors suggested using AIMD for frequency control of grid-connected microgrids. They considered both centralized and decentralized AIMD approaches and presented a comparison between those as well as with a PI-based controller. These studies assume that the congestion signal is delivered to the user by some mechanism without providing details on how it can be generated and implemented in the field. In [38], the authors suggest using the local voltages as a threshold for congestion signal in the AIMD algorithm. It is claimed that these thresholds can be extracted from historical voltage measurements for one time, however, without dynamic updates of thresholds, this approach will suffer from the lack of flexibility in adapting to changing conditions in the grid as expected with EV or photovoltaic solar integration. Using power flow analysis to calculate thresholds was suggested in [39], but this off-line solution cannot update itself to new real-time conditions. It is also important to note that none of these studies fully touch on the concept of charging fairness among customers, which is one of the main contributions of our work in this paper.

Decentralized operation of an AIMD-based EV charging algorithm relies on the measured and preset threshold voltage values. This makes it important to understand the effects of any system parameter on the node voltages. In this study, we present a detailed analysis regarding the relationship between distance versus voltage and power in a simplified distribution grid model [40]. This analysis shows that the proposed AIMD algorithm can achieve fair charging for EVs and avoid voltage violations provided that the voltage threshold values are set accordingly for each node depending on their locations in the grid. With this insight, we further focus on how to use local voltage measurements to estimate the grid congestion and set a voltage threshold value.

The degree of congestion in a power distribution grid can be estimated by the amount of voltage drop [41] similar to frequency-congestion relationship in power transmission

This article has been accepted for inclusion in a future issue of this journal. Content is final as presented, with the exception of pagination.

system. In this study, we further explore the EV integration impact on a low voltage distribution grid by means of statistical analysis [42]. We show that the statistical characteristics of voltage variations can be used as an input to our EV charging algorithm by providing congestion level information to control the charging.

Our contributions in this paper can be summarized as follows.

1) A relationship among voltage, power, and distance in a simplified distribution grid is derived.
2) A statistical analysis that verifies this relationship in a more realistic grid model is presented.
3) Based on the presented statistical analysis, a novel charging algorithm is proposed. This algorithm implements two-layer AIMD-based charging rate adaptation and provides an ability to learn threshold set points by local voltage measurements.
4) The fairness among EV owners is addressed, and the performance of the algorithm is evaluated in establishing proportional fairness among users.
5) The results of this study can provide crucial inputs for onboard residential and off-board dc fast charging operation control with the potential to be scaled to mass deployment of these infrastructure.

The organization of the paper is as follows. Section II presents the analytical derivation of voltage versus distance relationship. Section III introduces the model developed in MATLAB to test the analytical derivation. Section IV explains the AIMD-based proposed control methodology along with various case studies, and a discussion of the obtained results on the control methodology. Finally, Section V presents the conclusion and planned future work.

II. Analysis of Voltage Versus Distance Relationship

This section starts with deriving the relationship between the voltage of an end node and its distance from the substation analytically. Our goal is to gain insights on this relationship so that we can better guide the EV nodes for decentralized charging rate control. In this modeling effort, we use a simplified equivalent dc grid model as shown in Fig. 2.

This model uses a single mainline type primary distribution topology. It consists of one main feeder with voltages $V_1, V_2, \ldots, V_n$. There are n lateral feeders each with a total of k nodes. Each lateral node voltage is denoted as $V_{i1}, V_{i2}, \ldots, V_{ik}$ for the ith lateral node. Essentially, this model can be viewed as several repetitions of the lateral pattern given in Fig. 3. To find an analytical expression between the voltage of a main node and its distance from the substation, we model the main feeder in a repeated pattern. Then, the currents $I_1, I_2, \ldots, I_n$ in Fig. 3 represents the total currents drawn from each main node. To solve this repeated system for node voltages, we express each node voltage in terms of other system variables such that ith node voltage can be written as

$$V_i = V_0 - (I_1 + I_2 + \cdots + I_n)R_1 - (I_2 + \cdots + I_n)R_2 - (I_i + \cdots + I_n)R_i \quad (1)$$

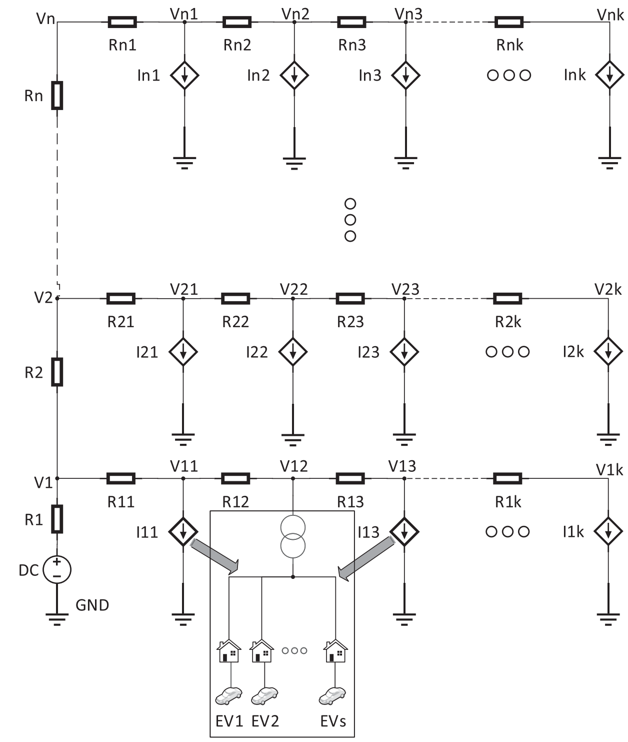

Fig. 2. Simple distribution grid model.

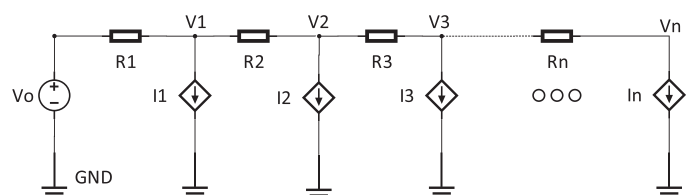

Fig. 3. Repeated pattern in the simple distribution system model.

where R_i is the resistance value of the line between ith and $(i-1)$th main nodes.

The voltage of any node in the grid is determined by the distribution line parameters and all the currents drawn at all nodes at any time. This results in a very complicated system without a simple analytic equation. However, one can formulate voltage versus distance relationship when the following assumptions hold true:

1) all currents are the same $I_1 = I_2 = I_3 = \cdots = I_n = I$;
2) all distribution line segment lengths and parameters are the same s.t. $R_1 = R_2 = R_3 = \cdots = R_n = \rho L/A$

where ρ is line resistivity ($\Omega\cdot$m), L is line segment length (m), A is line cross-sectional area (m^2) of the wire. Then, the voltage for ith node can be expressed as follows:

$$V_i = V_0 - \frac{I\rho L}{A}(n + (n-1) + (n-2) + \cdots + (n-i+1))$$

$$V_i = V_0 - \frac{I\rho L}{A}\left(\frac{2n-i+1}{2}i\right)$$

$$= V_0 - \frac{I\rho L}{A}\left(n + \frac{1}{2}\right)i + \frac{I\rho L}{A}\frac{i^2}{2}. \quad (2)$$

This article has been accepted for inclusion in a future issue of this journal. Content is final as presented, with the exception of pagination.

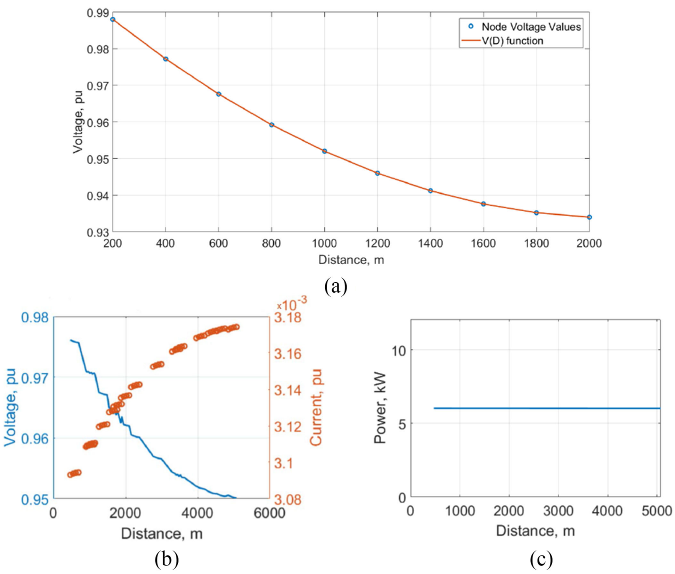

Fig. 4. (a) Relationship between main node voltages and their distances. (b) End-node voltages and currents wrt distance. (c) Fair allocation of charging power wrt distance.

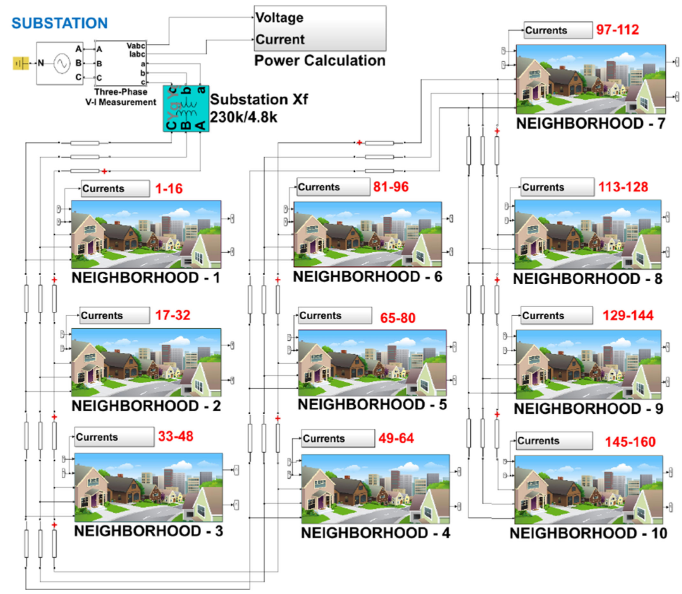

Fig. 5. MATLAB Simulink phasor model used for the low-voltage distribution grid.

By letting $D = Li$ (i being any node number), the voltage of the ith node can be defined as a function of its distance D from the substation as follows:

$$V\{D\} = V_0 - \frac{I\rho}{A}\left(n + \frac{1}{2}\right) D + \frac{I\rho}{A}\frac{D^2}{2L}. \tag{3}$$

Only with the presented assumptions, it is possible to represent this relationship by a quadratic function of a single variable (distance) as shown in (3). Fig. 4(a) shows the analytically computed voltages and the simulated voltages of ten main nodes of the repeated grid model in Fig. 3 when all nodes draw a constant current I equal to 0.02 p.u. This curve shows that even under simplified assumptions, the relationship between voltage and distance is not linear due to the complex topology of the grid.

In this study, our definition of ideal fairness in EVGI context is that every end node, regardless of its location, should draw the same charging power to maintain the same charging speed for every EV owner. However, the relationship in Fig. 4(a) shows that if every node draws the same current, the one with higher node voltage (or the one closer to the main feeder) will draw more power. For a fair charging strategy, the nodes should draw an inversely proportional charging current to its voltage. Ideally, the maximum possible amount of charging power for all nodes is achieved when the farthest end-node voltage is at the minimum utilization voltage level. The required end-node current values to ensure the same maximum power allocation to each node and the corresponding node voltages are computed and shown together in Fig. 4(b). The resulting currents increase as the voltages decrease to maintain the same power. The resulting power is approximately 6 kW for each node and this is shown with respect to distance in Fig. 4(c).

Although the simple grid model provides an important insight on voltage, current, and power relationships in terms of location, it does not truly represent the real grid system and cover real-life scenarios because of the presented assumptions and simplifications. Besides, working with fully analytic models in the real world is often times not possible or not convenient because of the stochastic nature of systems. This makes it necessary to carry out some statistical analysis to discover this nature. For all these reasons, a more realistic grid and load model are needed to carry this study to an upper level.

III. System Description for the Distribution Grid Test Case

In Section II, we used a single mainline type dc grid to analyze the voltage versus distance relationship. In this section, we convert this model to a more realistic three-phase ac grid structure that operates at a nominal voltage of 4.8 kV. We will use this grid structure as the benchmark for our EV charging study.

A. Distribution Grid Model

For our test benchmark, we designed a primary network in MATLAB Simulink as shown in Fig. 5. Each pictured box in Fig. 5 represents a neighborhood that is connected to a primary feeder bus. There are a total of ten neighborhoods located in ascending order of distance from the substation, i.e., first neighborhood is the closest and the tenth one is the farthest.

We model each neighborhood as a secondary network as shown in Fig. 6. The secondary network is developed following a similar procedure and data described in [43]. It contains four inner nodes and at each node, a pole-mounted transformer of 25 kVA is located. Each transformer steps down the primary feeder voltage of 4.8 kV to a secondary voltage level of 120/240 V and supplies power to four residential houses. In total, there are 160 residential customers in the model. The overall

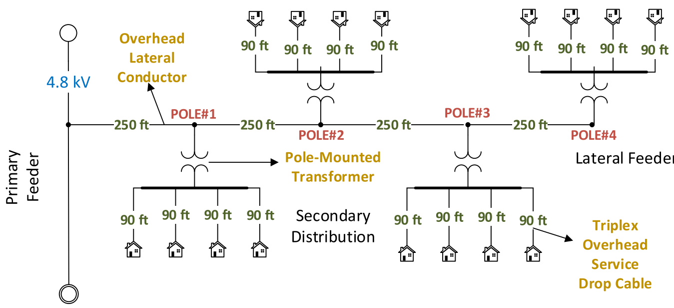

Fig. 6. Secondary distribution network structure implemented in the MATLAB model.

distribution grid operates slightly over 350 kW at peak hours without any charging event.

B. EV Load Model

In order to model EV charging load on the distribution grid, we focused on their critical parameters. We derived their arrival and departures times from a Gaussian distribution with mean and standard deviation of (5:30 P.M.,1 A.M.) and (07:47 A.M., 12:23 A.M.), respectively. The load model generates SOC values for each EV at the time of grid connection based on a Gaussian daily trip distribution with mean and standard deviation of (40.0 min, 5.0 min). Each EV is assumed to have a 60-kWh battery pack with an on-board charger of 7 kW corresponding to around 30-A ac current for a rated voltage of 240 V. The reason all the EVs are modeled with the same configuration type is to prevent possible confusions that might arise in the discussion of addressing fairness performance of the algorithm. We wanted to make sure the EVs' rate of charge do not interfere with the charging control algorithm's capability of attaining a fair charging scheme. Designing a charging control algorithm that can attain fairness across heterogeneous EVs with different capabilities is a future direction our work can be taken to.

C. Residential Load Model

We designed a random consumption data generator for residential houses. The power consumption profile for each house in the simulation model are generated using 16 d of real power consumption data of a household collected by e-Gauge [44] at 1-min intervals (see Fig. 7). For each 1-min interval, the 16 d of data specific to that interval period are used to model the power consumption as a Gaussian distributed random variable where the mean and variance parameters of the distribution are calculated from the e-Gauge data for that interval. By this way, a different power consumption probability distribution function (PDF) is defined for each time interval of a day. Hence, simulation of power consumption of an house for each time interval is done by generating a random value from the corresponding PDF for that time interval. One example of such a profile is shown in Fig. 8. We then assumed 0.9 power factor lagging operation by keeping the active power consumption the same since the original e-Gauge data did not include reactive power consumption which is very common in residential houses.

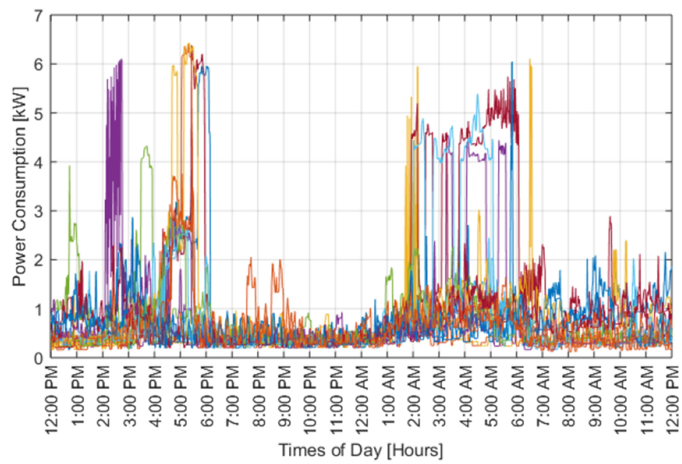

Fig. 7. Sixteen days (shown in different colors) of power consumption data of a household.

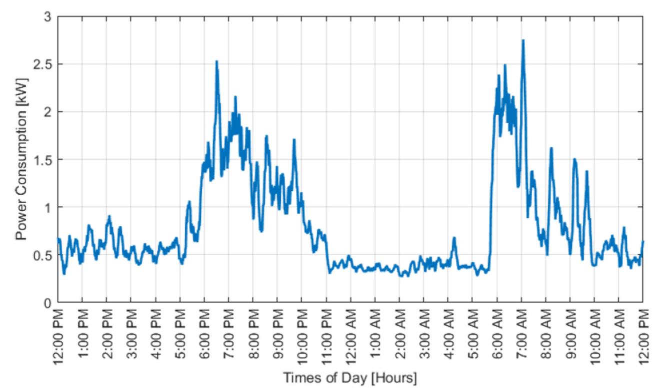

Fig. 8. Sample power profile of a single household generated from 16 d of consumption data.

D. Verification of the Analytic Model Through Statistical Analysis

To verify the voltage and distance relationship presented in Section II through statistical analysis, a Monte Carlo simulation is developed. The realistic grid model in Fig. 5 is simulated for a period of 100 d and phase voltages of the main nodes are recorded for the interval of 6:00–6:15 P.M. at 1-min intervals, which create a total of 1500 data samples. The average of these simulated phase voltages are then compared with the voltage values computed by (3), and the results are shown in Fig. 9.

This comparison assumes that the distribution lines are purely resistive and the currents drawn from each neighborhood are equal on average. The distribution grid data for this analysis is extracted from IEEE 37-Node Test Feeder [45]. Using this dataset, we considered each line segment with $R = 2.09\ \Omega$ and $X = 0.77\ \Omega$. Since $R \approx Z$, neglecting X in the analysis gives a negligible error. The statistical analysis developed here considered X as well and showed that both analysis demonstrated a similar relationship as shown in Fig. 9. The reason that the analytically computed voltages are little higher than the measured ones is because the presented assumptions ignore the voltage drops due to the line inductances.

This article has been accepted for inclusion in a future issue of this journal. Content is final as presented, with the exception of pagination.

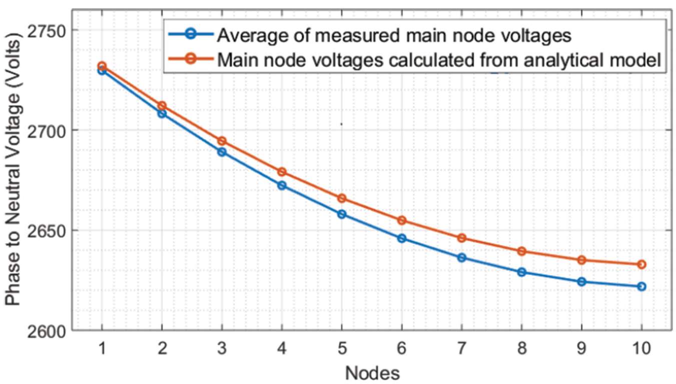

Fig. 9. Comparison between measured and analytically obtained main node voltages.

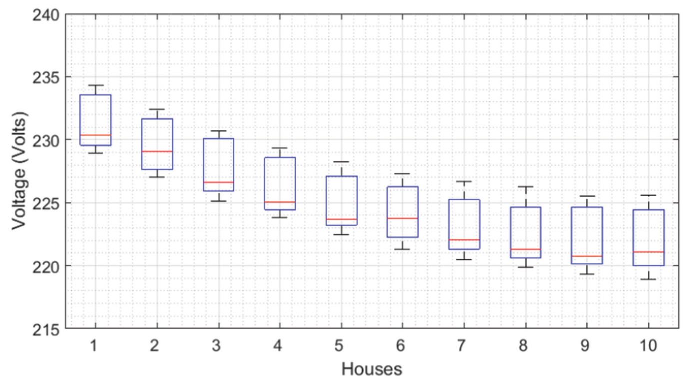

Fig. 10. Box plot of voltages averaged over 6:00–6:15 P.M. for ten houses after 100 d at full charging power.

Algorithm 1: Proposed AIMD Algorithm.

Input: Charger voltage and current: $V_c(t)$, $I_c(t)$
Output: Charger current command $I_c(t+1)$
if $V_c(t) > V_{th}(t)$ **then**
$I_c(t+1) = I_c(t) + \alpha(t)$
else
$I_c(t+1) = \beta(t) \times I_c(t)$
end if

IV. Proposed AIMD-Based EV Charge Control Algorithm

A. Baseline Algorithm With Learning Threshold Voltages

In this section, the AIMD algorithm is adopted into the EV charging control. The baseline implementation of this algorithm is explained in Algorithm 1. This algorithm either increases or decreases the charging current, thus charging power, depending on whether or not its node voltage $V_c(t)$ exceeds its threshold voltage $V_{\text{th}}(t)$. Increase is done additively by $\alpha(t)$, whereas decrease is done by the multiplicative factor $\beta(t)$. Here $V_{\text{th}}(t)$ is the key parameter since it serves as a congestion indicator. The minimum and maximum utilization voltage ranges are specified as 0.9 and 1.05 p.u. by ANSI C84.1-2016. These values correspond to 216 and 252 V for 240-V nominal voltage. The algorithm can also be modified to take these limits into account. Two additional fix thresholds being the lower and upper voltage limits can be introduced to the detection condition. Thereby, the AIMD algorithm takes action not only in the case of network congestion, but also of voltage limit violations, by either reducing or increasing the charging power.

The voltage level at a certain point in the grid varies depending not only on the grid structure and distribution line lengths, but also on the overall system load at any time. Therefore, $V_{\text{th}}(t)$ must be specific to each node such that observing this specific voltage and comparing with node's regular voltage profile should reveal the congestion event information. This implies that the distant locations with respect to the substation should have lower threshold values compared to closer nodes since they experience lower voltages. Consequently, there should be a correlation between the threshold value of a node and its voltage profile. The voltage profile itself also changes in accordance with the loading level of the grid over a day. Therefore, it must be defined as a function of time. For a given time interval, this profile follows a normal distribution based on the results of our measurements. The mean of the distribution represents the general tendency of the voltage, whereas the variance means how much the node voltage is effected by the load changes in the grid.

Our previous work discusses how voltage profiles vary at different EV penetration levels and how to obtain the voltage distributions with respect to nodes [42]. After learning the distribution for time intervals, we can set our threshold to the value which corresponds to the 25th percentile of the distribution. This will give the node some voltage margin to drop below its mean value. Since the threshold value is directly derived from the node's voltage profile, it also adapts itself to any change in the grid by constantly relearning the voltage distribution. This should be highlighted as a key ability of the proposed algorithm.

B. Implementation of Baseline Algorithm

This section shows whether the statistically learned threshold voltages can result in fair average charging power among customers regardless of their location in the grid. Initially, it is assumed that only 16 households (10% penetration) have EVs. For 100 d of simulation, the EVs are charged at rated fixed power of 7.2 kW, and their node voltages were recorded. The distribution of the recorded voltages of ten selected houses from each neighborhood is shown as box plots in Fig. 10 in ascending order of distance. As it can be seen, the voltage distributions decrease as the distance of the house from the substation increases and the downward trend is not linear, but rather of a quadratic form.

Each voltage distribution is calculated by only the local voltage values observed at that house. Each box in Fig. 10 corresponds to a different house, and each house can calculate its own voltage threshold without any further information from

This article has been accepted for inclusion in a future issue of this journal. Content is final as presented, with the exception of pagination.

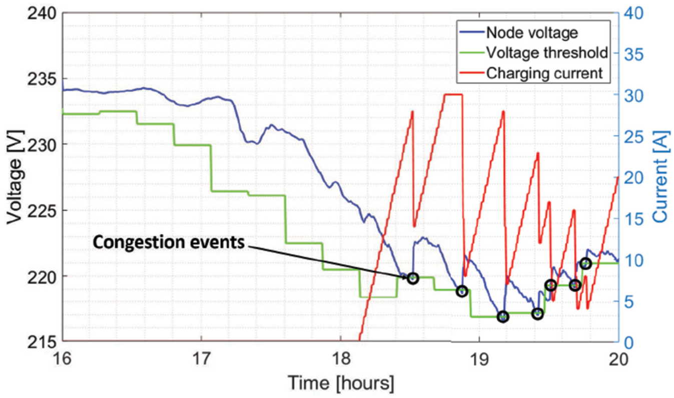

Fig. 11. Node voltage, voltage threshold, and charging current waveforms of a single vehicle as AIMD is in action.

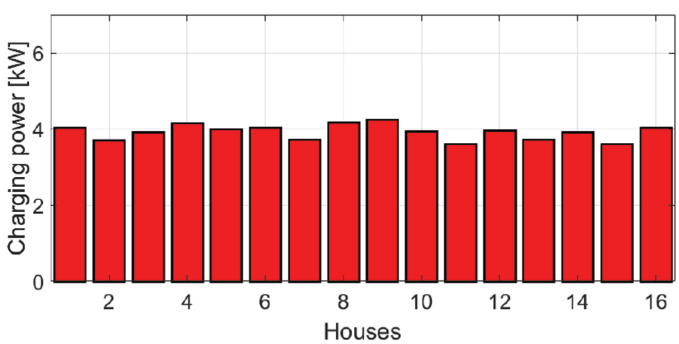

Fig. 12. Average EV charging powers at 10% penetration after the implementation of AIMD with learned threshold values.

other houses. A voltage threshold that represents 25th percentile is selected for each house.

Later, 100 simulations were re-run with the learned threshold voltages, but this time, the EVs implemented Algorithm 1 ($\alpha = 1$ and $\beta = 0.5$) rather than charging at the rated power rate. To demonstrate the operation of the algorithm, Fig. 11 shows voltage profile, charging current, and voltage threshold waveforms over the time period of 4:00–8:00 P.M. for a single EV. The congestion events occur when the node voltage drops below the calculated threshold values. They are demonstrated by black circles in the figure. The current linearly increases until the node voltage becomes lower than the threshold (congestion event) during when it is multiplicative reduced. The resulting average charging power of 16 houses (10% penetration) are shown Fig. 12. As shown, EVs learned to charge at approximately 4 kW of power without needing any central charging power command and only by using local voltage information. However, this case only implemented a single learning cycle and showed that some degree of fairness has been established through statistically learning of voltage thresholds and using them in the AIMD algorithm.

The problem with this approach is that as every node constantly learns their thresholds and uses them in the AIMD, their average charging power gradually decreases in favor of the grid. This will create an upward trend in the measured local voltages

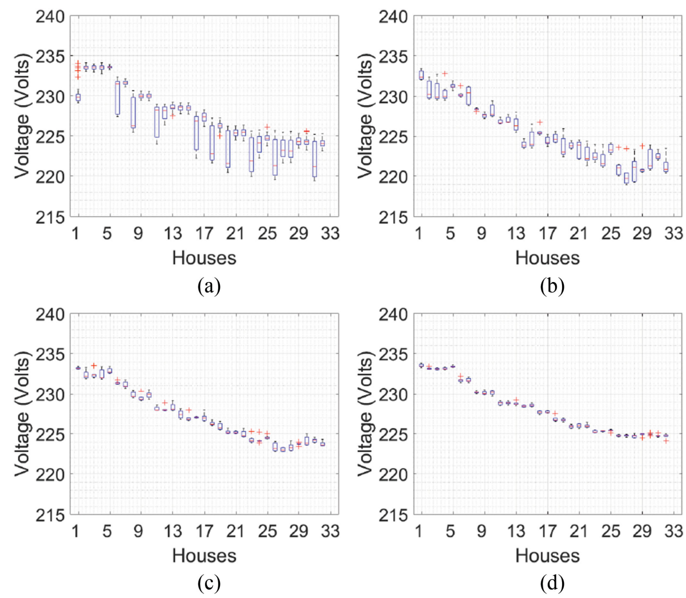

Fig. 13. Box plot representation of 32 end-node voltages between (20% penetration) 6:00–6:15 P.M. after (a) 1st week, (b) 3rd week, (c) 6th week, and (d) 10th week.

causing the threshold values to go even higher. This is demonstrated with a case study described as follows. It is assumed that the first 16 EVs in the first case already know their thresholds and another set of 16 EVs are integrated into the grid making with the total penetration level 20%. This scenario investigates whether a fairness will be established between the former and latter 10% EV populations by constantly learning and updating their thresholds.

The recently integrated EVs will start their learning process by charging at the fixed rated power of 7.2 kW and will then start implementing the AIMD after they learn their first thresholds over 7 d. Figs. 13 and 14 show the voltage distributions and average charging powers of 32 end nodes between 6:00–6:15 P.M. after 1st week, 3rd week, 6th week, and 10th week, respectively. As seen, the voltage distributions always move upward causing the thresholds to increase as well. This results in the average charging powers decreasing after every learning cycle. Higher threshold means lower average power compared to lower threshold. So, in the long run, the system will always try to heal itself by lowering the charging powers toward zero, essentially causing a slow charging speed problem.

C. Voltage Threshold Update Algorithm

To solve this problem, a threshold update algorithm is proposed in this study. This algorithm is executed after the learning process is completed. It compares the new estimated threshold value with the previous one. If the threshold has increased, then it lowers it by a constant voltage value, i.e., $k > 0$. If the threshold has dropped or stayed the same, it does not take any action because this indicates that the system has already sufficient voltage margin to use. The threshold update algorithm is defined in Algorithm 2.

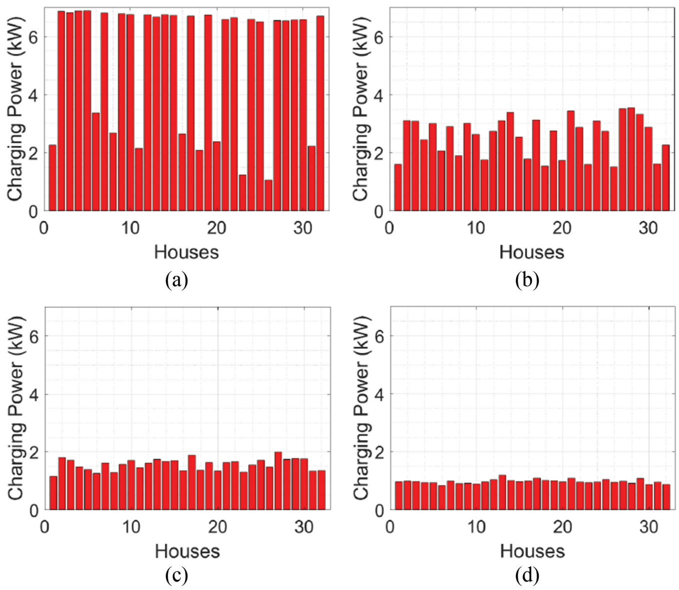

Fig. 14. Average charging power of EVs (20% penetration) for (a) 1st week, (b) 3rd week, (c) 6th week, and (d) 10th week. (Single-layer AIMD).

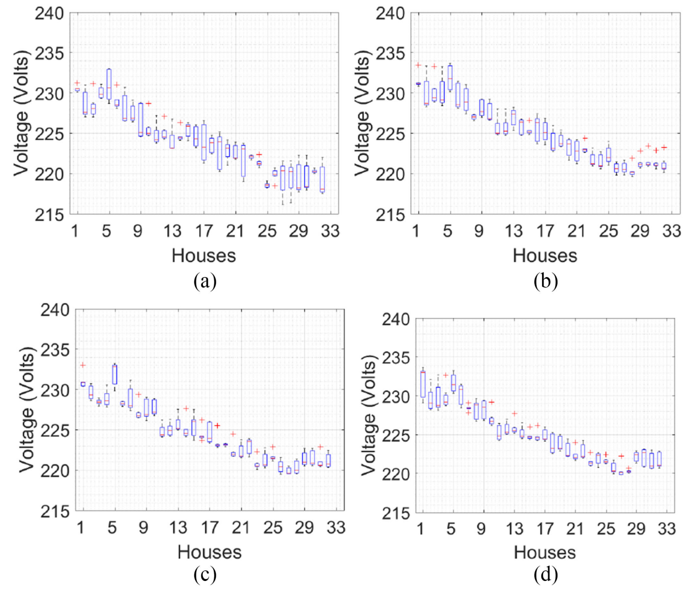

Fig. 16. Box plot representation of 32 end-node voltages (20% penetration) between 6:00–6:15 P.M. for (a) 1st week, (b) 10th week, (c) 20th week, and (d) 30th week. (Two-layer AIMD).

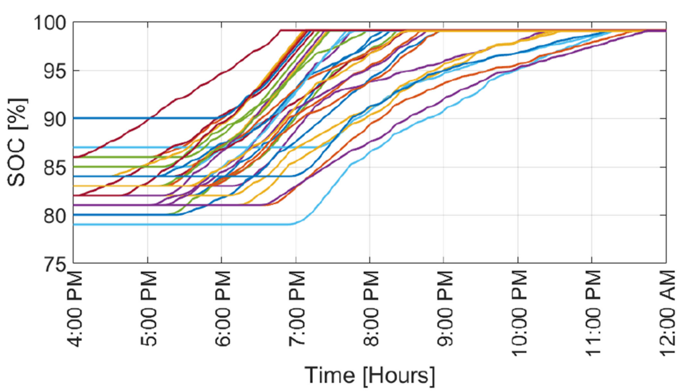

Fig. 15. SOC variations of 32 vehicles (20% penetration) over the time period between 4:00 P.M.–12:00 A.M.

Algorithm 2: Proposed Voltage Threshold Update Algorithm.

Input: Previous and new thresholds: $V_{\text{th(prev)}}, V_{\text{th(new)}}$
Output: Final threshold : $V_{\text{th(final)}}$
  if $V_{\text{th(new)}} > V_{\text{th(prev)}}$ **then**
    $V_{\text{th(final)}} = V_{\text{th(new)}} - k$
  else
    $V_{\text{th(final)}} = V_{\text{th(prev)}}$
end if

D. Implementation of the Advanced Algorithm

To overcome the self-healing problem mentioned in Section IV-B, the vehicles will also implement Algorithm 2 in this case study. The voltage reduction constant (k) is of significant importance since it effects the average charging power of each EV. Thus, the ideal value of k for a given system greatly depends on the available capacity and topology constraints. In this study, k was experimentally adjusted to be 1.25 V so that the average charging power converges around a moderate value for each vehicle. Also, the voltage at the farthest node stays slightly over the critical voltage threshold.

The learning time that is needed to collect the measured data and generate the associated voltage distributions was chosen to be one week as it could generate enough data samples for learning. In this way, the system will be able to capture changes in the grid operation in a short time frame. The whole simulation is run for 100 weeks to evaluate how the fairness is maintained in the long run. The voltage distributions and the average charging power for each household in the 1st, 10th, 20th, and 30th weeks are given in Figs. 16 and 17, respectively. The SOC variations of all 32 vehicles (20%) over the period between 4:00 P.M.–12:00 A.M. are shown in Fig. 15. This figure shows that all EVs manage to achieve their energy demand before 12:00 A.M.

The application of the AIMD algorithm in the EV charging problem has several important objectives. These include utilizing the maximum available capacity system to charge EVs as fast as possible, avoiding any voltage violations, and establishing fairness among vehicle owners.

Once the threshold values are determined properly, the proposed AIMD algorithm establishes a proportional fairness resulting in approximately equal average charging powers (see Fig. 12). However, due to the dynamic nature of the grid as in the case with the Internet, the load level may gradually increase as new EVs are connected to the system. This requires adapting voltage thresholds periodically. The length of this period was chosen in this study to be 7 d.

The results of Algorithm 2 have shown that even though there is a significant increase in the EV penetration, since all EVs learn new thresholds, their average charging powers reached an

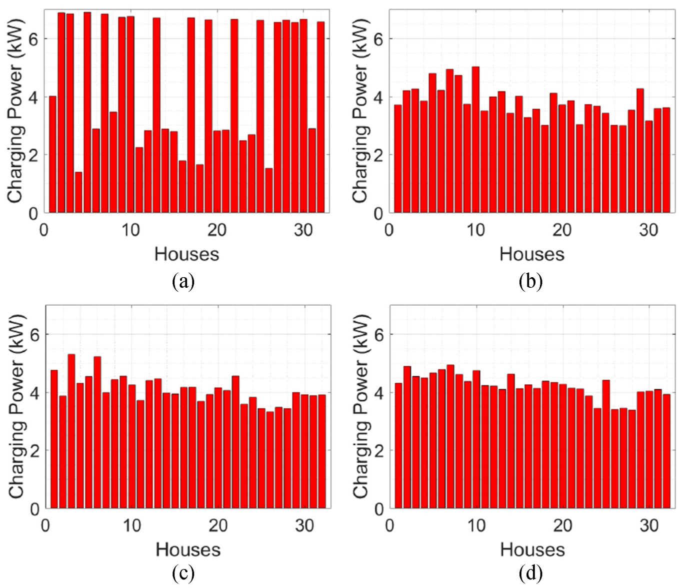

Fig. 17. Average charging power of EVs (20% penetration) for (a) 1st week, (b) 10th week, (c) 20th week, and (d) 30th week. (Two-layer AIMD).

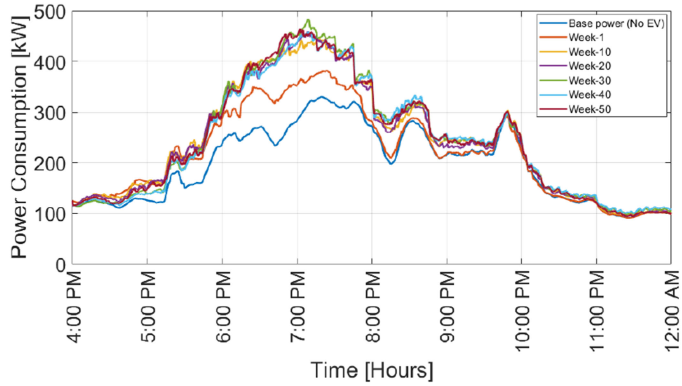

Fig. 18. Total power of the system along with the base power (no EV) in 1st, 10th, 20th, 30th, 40th, and 50th weeks between 4:00–12:00 P.M. interval.

equilibrium point around 4 kW (see Fig. 17). This equilibrium point is determined by the constant voltage parameter k of Algorithm 2. A higher k value will shift the equilibrium point upward since it decreases the thresholds allowing the charging currents to increase even more.

Equilibrium state can also be observed from the voltage distributions in Fig. 16. After 20th week, the voltage distributions converge to an equilibrium point for each node within a tight voltage interval. This result shows that a charging operating point for each EV can be set by adjusting a single parameter, i.e., k.

The obtained results showed that each local observed voltage distribution carries information about the congestion and can be successfully used in the learning process for the EV charging control. It can also be inferred that the reduction parameter k being the same at all nodes could bring some more advantages for those nodes which are closer to the substation or experience high voltage profiles. This is because it takes more power for the closer nodes to see the same amount of voltage drop compared to the further nodes. One possible solution for this would be adjusting the reduction parameter k in accordance with the voltage profile just like in the case of thresholds. This will assign slightly higher k values to the far-end nodes relative to the closer nodes. In the future, we will work to further improve these ideas and also try to develop a method to determine the k parameter.

The total power of the system in 1st, 10th, 20th, 30th, 40th, and 50th weeks between 4:00–12:00 P.M. is shown in Fig. 18. This figure shows that the total power has reached a peak value after the 20th week and stayed around this power in the following weeks. This validates the results shown in Fig. 17 showing that the average charging powers of the EVs reached an equilibrium point. This settling time is dependent on how frequently threshold values are calculated. In this study, every node updated their thresholds every week. If we reduce this time, the system can more quickly settle around a charging power. It is also seen in this figure that the overall charging power shifted toward the 7:00–8:00 P.M. interval as weeks pass. This naturally happens as more EVs implement the AIMD algorithm.

V. CONCLUSION

Inspired by the operation of the Internet, this paper develops a novel decentralized, stable, fair, and practical EV charging solution. Thereby, the AIMD control algorithm, the main protocol for TCP, is adopted and modified in this paper for EV charging via learning the threshold voltages of individual charging nodes. The value of the threshold voltage depends on the EV location as well as EV penetration ratio in the system. In this paper, we proposed a novel method to determine the threshold voltages based on the statistically collected local voltage values providing a decentralized control solution.

For future studies, the proposed algorithms will be further improved and tested for more realistic grid structures. It is also stated in the paper that a single parameter k establishes fairness among users, but at which power level it should achieve the fairness is now a new current direction and requires some capacity estimation methods with available local information. A hardware environment will be developed where the behavior of a grid is simulated in real time by a grid simulator and the charging algorithms are implemented on hardware via real power converters. Installing charging infrastructures in the field and collecting real-time voltage, current, and power data in the event of EV charging will also help us better understand the relationships among these parameters and be definitely a future direction to go.

REFERENCES

[1] Electric Vehicle Outlook 2017. (2017). [Online]. Available: https://data.bloomberglp.com/bnef/sites/14/2017/07/BNEF_EVO_2017_ExecutiveSummary.pdf

[2] K. Knezović, M. Marinelli, A. Zecchino, P. B. Andersen, and C. Traeholt, “Supporting involvement of electric vehicles in distribution grids: Lowering the barriers for a proactive integration,” *Energy*, vol. 134, pp. 458–468, 2017.

[3] F. Erden, M. C. Kisacikoglu, and O. H. Gurec, "Examination of EV-grid integration using real driving and transformer loading data," in *Proc. Int. Conf. Elect. Electron. Eng.*, 2015, pp. 364–368.
[4] L. P. Fernandez, T. G. San Roman, R. Cossent, C. M. Domingo, and P. Frías, "Assessment of the impact of plug-in electric vehicles on distribution networks," *IEEE Trans. Power Syst.*, vol. 26, no. 1, pp. 206–213, Feb. 2011.
[5] S. Shafiee, M. Fotuhi-Firuzabad, and M. Rastegar, "Investigating the impacts of plug-in hybrid electric vehicles on power distribution systems," *IEEE Trans. Smart Grid*, vol. 4, no. 3, pp. 1351–1360, Sep. 2013.
[6] E. Veldman and R. A. Verzijlbergh, "Distribution grid impacts of smart electric vehicle charging from different perspectives," *IEEE Trans. Smart Grid*, vol. 6, no. 1, pp. 333–342, Jan. 2015.
[7] E. Sortomme, M. M. Hindi, S. J. MacPherson, and S. Venkata, "Coordinated charging of plug-in hybrid electric vehicles to minimize distribution system losses," *IEEE Trans. Smart Grid*, vol. 2, no. 1, pp. 198–205, Mar. 2011.
[8] N. Leemput, F. Geth, J. Van Roy, A. Delnooz, J. Buscher, and J. Driesen, "Impact of electric vehicle on-board single-phase charging strategies on a flemish residential grid," *IEEE Trans. Smart Grid*, vol. 5, no. 4, pp. 1815–1822, Jul. 2014.
[9] K. Clement-Nyns, E. Haesen, and J. Driesen, "The impact of charging plug-in hybrid electric vehicles on a residential distribution grid," *IEEE Trans. Power Syst.*, vol. 25, no. 1, pp. 371–380, Feb. 2010.
[10] O. Sundstrom and C. Binding, "Flexible charging optimization for electric vehicles considering distribution grid constraints," *IEEE Trans. Smart Grid*, vol. 3, no. 1, pp. 26–37, Mar. 2012.
[11] D. Dallinger, R. Kohrs, S. Marwitz, and J. Wesche, Plug-In Electric Vehicles Automated Charging Control. (2015). [Online]. Available: http://publica.fraunhofer.de/documents/N-327920.html
[12] B. Li, M. C. Kisacikoglu, C. Liu, N. Singh, and M. Erol-Kantarci, "Big data analytics for electric vehicle integration in green smart cities," *IEEE Commun. Mag.*, vol. 55, no. 11, pp. 19–25, Nov. 2017.
[13] M. J. E. Alam, K. M. Muttaqi, and D. Sutanto, "A controllable local peak-shaving strategy for effective utilization of PEV battery capacity for distribution network support," *IEEE Trans. Ind. Appl.*, vol. 51, no. 3, pp. 2030–2037, May/Jun. 2015.
[14] S. Deilami, A. S. Masoum, P. S. Moses, and M. A. Masoum, "Real-time coordination of plug-in electric vehicle charging in smart grids to minimize power losses and improve voltage profile," *IEEE Trans. Smart Grid*, vol. 2, no. 3, pp. 456–467, Sep. 2011.
[15] M. C. Kisacikoglu, M. Kesler, and L. M. Tolbert, "Single-phase on-board bidirectional PEV charger for V2G reactive power operation," *IEEE Trans. Smart Grid*, vol. 6, no. 2, pp. 767–775, Mar. 2015.
[16] A. T. Al-Awami, E. Sortomme, G. M. A. Akhtar, and S. Faddel, "A voltage-based controller for an electric-vehicle charger," *IEEE Trans. Veh. Technol.*, vol. 65, no. 6, pp. 4185–4196, Jun. 2016.
[17] M. C. Kisacikoglu, F. Erden, and N. Erdogan, "Distributed control of PEV charging based on energy demand forecast," *IEEE Trans. Ind. Inform.*, vol. 14, no. 1, pp. 332–341, Jan. 2018.
[18] V. Jacobson, "Congestion avoidance and control," in *Proc. Conf. Appl. Technol. Architectures, Protocols Comput. Commun.*, Aug. 1988, pp. 314–329.
[19] S. Floyd, "Congestion control principles," *in Internet Engineering Task Force Requests for Comments 2914*. Reston, VA, USA: Internet Society, Sep. 2000.
[20] J. Nagle, "Congestion control in IP/TCP internetworks," *Internet Engineering Task Force Requests for Comments 896*, Ford Aerospace and Communications Corporation, Jan. 1984.
[21] D. M. Chiu and R. Jain, "Analysis of the increase/decrease algorithms for congestion avoidance in computer networks," *J. Comput. Netw. ISDN Syst.*, vol. 17, no. 1, pp. 1–14, Jun. 1989.
[22] M. Allman, V. Paxson, and E. Blanton, "TCP congestion control," *in IETF RFC 5681*, Network Working Group, Purdue Univ., West Lafayette, IN, USA, Sep. 2009.
[23] H. Balakrishnan and S. Seshan, "The congestion manager," in *Internet Engineering Task Force Requests for Comments 3124*. Network Working Group, Carnegie Mellon Univ., Pittsburgh, PA, USA, Jun. 2001.
[24] S. Kunniyur and R. Srikant, "End-to-end congestion control schemes: Utility functions, random losses and ECN marks," *IEEE/ACM Trans. Netw.*, vol. 11, no. 5, pp. 689–702, Oct. 2003.
[25] S. H. Low and D. E. Lapsley, "Optimization flow control—I: Basic algorithm and convergence," *IEEE/ACM Trans. Netw.*, vol. 7, no. 6, pp. 861–875, Dec. 1999.
[26] R. Shorten, D. Leith, and P. Wellstead, "An adaptive AIMD congestion control protocol for communication networks," in *Networking*. Berlin, Heidelberg, Germany: Springer, 2004, pp. 699–711.
[27] P. Hurley, J.-Y. Le Boudec, and P. Thiran, "A note on the fairness of additive increase and multiplicative decrease," in *Proc. ITC-16*, 1999, pp. 1–12.
[28] M. Corless, C. King, R. Shorten, and F. Wirth, *AIMD Dynamics and Distributed Resource Allocation*. Philadelphia, PA, USA: Soc. Ind. Applied Math., 2016.
[29] A. A. Abouzeid, S. Roy, and M. Azizoglu, "Stochastic modeling of TCP over lossy links," in *Proc. INFOCOM*, 2000, pp. 1724–1733.
[30] S. Studli, E. Crisostomi, R. Middleton, and R. Shorten, "AIMD-like algorithms for charging electric and plug-in hybrid vehicles.," in *Proc.Int. Elect. Veh. Conf.*, Mar. 2012, pp. 1–8.
[31] S. Studli, R. H. Khan, R. H. Middleton, and J. Y. Khan, "Performance analysis of an AIMD based EV charging algorithm over a wireless network," in *Proc. Australas. Univ. Power Eng. Conf.*, 2013, pp. 1–6.
[32] S. Stüdli, E. Crisostomi, R. Middleton, and R. Shorten, "A flexible distributed framework for realising electric and plug-in hybrid vehicle charging policies," *Int. J. Control*, vol. 85, pp. 1130–1145, 2012.
[33] M. Liu and S. McLoone, "Enhanced AIMD-based decentralized residential charging of EVs," *Trans. Inst. Meas. Control*, vol. 37, no. 7, pp. 853–867, 2015.
[34] I. Beil and I. Hiskens, "Coordinated PEV charging and its effect on distribution system dynamics," in *Power Syst. Comput. Conf.*, Aug. 2014, pp. 1–7.
[35] M. Liu, P. McNamara, and S. McLoone, "Fair charging strategies for EVS connected to a low-voltage distribution network," in *Proc. IEEE PES Innovative Smart Grid Technol. Europe*, Oct. 2013, pp. 1–5.
[36] E. Crisostomi, M. Liu, M. Raugi, and R. Shorten, "Plug-and-play distributed algorithms for optimized power generation in a microgrid," *IEEE Trans. Smart Grid*, vol. 5, no. 4, pp. 2145–2154, Jul. 2014.
[37] P. Ferraro, E. Crisostomi, R. Shorten, and F. Milano, "Stochastic frequency control of grid-connected microgrids," *IEEE Trans. Power Syst.*, vol. 33, no. 5, pp. 5704–5713, Sep. 2018.
[38] L. Xia, I. Mareels, T. Alpcan, M. Brazil, J. de Hoog, and D. A. Thomas, "A distributed electric vehicle charging management algorithm using only local measurements," in *Proc. Innovative Smart Grid Technol.*, Feb. 2014, pp. 1–5.
[39] M. J. Zangs, P. B. E. Adams, T. Yunusov, W. Holderbaum, and B. A. Potter, "Distributed energy storage control for dynamic load impact mitigation," *Energies*, vol. 9, no. 8, p. 647, 2016.
[40] E. Ucer, M. C. Kisacikoglu, and M. Yuksel, "Analysis of an Internet-inspired EV charging network in a distribution grid," in *Proc.IEEE/PES Transmiss. Distribution Conf. Expo.*, 2018, pp. 1–5. [Online]. Available: http://mck.people.ua.edu/uploads/8/7/7/8/87787552/ucer_t_d_paper.pdf
[41] N. O'Connell, Q. Wu, J. stergaard, A. Nielsen, S. Cha, and Y. Ding, "Day-ahead tariffs for the alleviation of distribution grid congestion from electric vehicles," *Electric Power Syst. Res.*, vol. 92, pp. 106–114, 2012.
[42] E. Ucer, M. C. Kisacikoglu, and A. Gurbuz, "Learning EV integration impact on a low voltage distribution grid," in *Proc. IEEE Power Energy Soc. General Meeting*, 2018, pp. 1–5. [Online]. Available: http://mck.people.ua.edu/uploads/8/7/7/8/87787552/pes_gm_ucer_2018.pdf
[43] A. R. Malekpour and A. Pahwa, "Radial test feeder including primary and secondary distribution network," in *Proc. North Amer. Power Symp.*, Oct. 2015, pp. 1–9.
[44] Energy Monitoring Systems for Residential and Commercial Applications. (2018). [Online]. Available: http://www.egauge.net/
[45] IEEE PES AMPS DSAS Test Feeder Working Group. (2018). [Online]. Available: http://sites.ieee.org/pes-testfeeders/resources/

Emin Ucer (S'18) received the B.S. degree in electrical and electronics engineering from Hacettepe University, Ankara, Turkey, in 2015. He has been working toward the Ph.D. degree at the University of Alabama, Tuscaloosa, AL, USA, since January 2017.

He has worked as a Research Engineer with TUBITAK between 2015 and 2016. His research interests include power electronics, electric vehicles (EVs), EV-grid integration and control, and machine learning and artificial intelligence based techniques and their applications.

Mithat C. Kisacikoglu (S'04–M'14) received the Ph.D. degree in electrical engineering from the University of Tennessee, Knoxville, TN, USA, in 2013.

He has worked with National Renewable Energy Laboratory, Golden, CO, USA, as a Research Engineer between 2015 and 2016. He is currently an Assistant Professor with the Electrical and Computer Engineering Department at University of Alabama, Tuscaloosa, AL, USA. His research interests include electric vehicles, EV-grid integration, and power electronics converters.

Murat Yuksel (SM'11) received the Ph.D. degree in computer science from Rensselaer Polytechnic Institute, Troy, NY, USA, in 2002.

Until 2016, he was with the CSE Department of the University of Nevada, Reno, NV, USA, as a faculty member. He is currently an Associate Professor with the ECE Department of the University of Central Florida (UCF), Orlando, FL, USA. His research interests include networked, wireless, and computer systems.

Ali Cafer Gurbuz (M'08–SM'18) received the Ph.D. degree in electrical and computer engineering from Georgia Institute of Technology, Atlanta, GA, USA, in 2008.

He held faculty positions with TOBB University, Ankara, Turkey, and University of Alabama, Tuscaloosa, AL, USA, between 2009 and 2017. Currently, he is an Assistant Professor with the Department of Electrical and Computer Engineering at Mississippi State University, MS, USA. His research interests include development of sparse signal representations, compressive sensing theory and applications, radar and sensor array signal processing, and machine learning.